Pediatric Radiology (2021) 51:353–370
https://doi.org/10.1007/s00247-020-04794-y

REVIEW

Superficial anatomy of the neonatal cerebrum — an ultrasonographic roadmap

Fabrício Guimarães Gonçalves[1] · Misun Hwang[2]

Received: 26 March 2020 / Revised: 6 July 2020 / Accepted: 4 August 2020 / Published online: 7 October 2020

Abstract

Neurosonography is an essential imaging modality for assessing the neonatal brain, particularly as a screening tool to evaluate intracranial hemorrhage, hydrocephalus and periventricular leukomalacia. The primary advantages of neurosonography include portability, accessibility and lack of ionizing radiation. Its main limitations are intrinsic operator dependence and the need for an open fontanelle. Neurosonographic imaging acquisition is typically performed by placing a sector transducer over the anterior fontanelle and following sagittal and coronal sweeps. The sensitivity of neurosonography has markedly improved thanks to the adoption of modern imaging equipment, the use of dedicated head probes, and the employment of advanced diagnostic US techniques. These developments have facilitated more descriptive identification of specific cerebral anatomical details, improving understanding of the cerebral anatomy by conventional US. Such knowledge is fundamental for enhanced diagnostic sensitivity and is a key to understanding pathological states. Furthermore, familiarity with normal anatomy is crucial for understanding pathological states. Our primary goal in this review was to supplement these technological developments with a roadmap to the cerebral landscape. We accomplish this by presenting a systematic approach to using routine US for consistent identification of the most crucial cerebral landmarks, reviewing their relationship with adjacent structures, and briefly describing their primary function.

Keywords Anatomy · Brain · Neonate · Neurosonography · Ultrasound

Neurosonography

Indications

Neurosonography is an essential imaging modality used to evaluate the neonatal brain [1], mainly as a screening tool in the assessment of intracranial hemorrhage (i.e. germinal matrix hemorrhage), hydrocephalus and periventricular leukomalacia [2]. Neurosonography screening can also be performed (with varying degrees of sensitivity and specificity) in cases of abnormal head circumference and vascular abnormalities; in children under hypothermia treatment, on extracorporeal membrane oxygenation support or other support machines; cases of congenital malformations, seizures, intrauterine growth restriction, congenital or acquired brain infection and suspected or known head trauma; and for follow-up or surveillance of previously documented abnormalities, including prenatal abnormalities [3].

Advantages and limitations

The main advantages of diagnostic US include portability, accessibility and lack of ionizing radiation [4, 5]. In particular, with neurosonography, a comprehensive evaluation of the neonatal brain can be performed at the bedside with no need for sedation and with minimal preparation [6]. Moreover, neurosonography is a noninvasive modality that can be performed in neurologically ill infants without the risks associated with transportation and neck manipulation [4, 5].

One relevant limitation of US is its intrinsic high operator dependence, mostly related to variable technical skills in obtaining images, knowledge of the US system capabilities (knobology), training, experience, and understanding of the

✉ Misun Hwang
hwangm@email.chop.edu

[1] Division of Neuroradiology, Department of Radiology, Children's Hospital of Philadelphia, Philadelphia, PA, USA

[2] Department of Radiology, Children's Hospital of Philadelphia, University of Pennsylvania, 3401 Civic Center Blvd., Philadelphia, PA 19104, USA

anatomy, physiology and pathological changes of the brain [7]. Inherent limitations specific to neurosonography include the limited overview of the posterior fossa (which can be overcome by the adoption of mastoid/posterior fontanelle views), cortical regions and convexity of the brain; lack of standardized parameters to assess the myelination process; as well as reduced sensitivity and specificity in the evaluation of brain ischemia, white matter disorders, metabolic diseases and complex brain malformations [2, 5, 8–12]. If an abnormality is found or suspected on US, this can lead to a recommendation for advanced imaging with MRI or CT, with a greater degree of yield, which could be more important in critically ill infants.

Neurosonography imaging acquisition

Equipment

The preferred probes for neurosonography are sector or linear-array transducers, which can adjust and capture images through the anterior fontanelle [3]. While sector transducers allow for a wider field of view, linear-array transducers have a higher frequency and therefore are recommended for evaluating superficial structures or lesions. These include extra-axial collections, venous thrombosis, cerebral edema, and gyral–sulcal anatomy, such as in suspected migrational anomalies [13]. Although linear transducers might help resolve the compartment that an extra-axial fluid collection occupies as long as it is near the midline, they are less useful for collections over the convexities, where the sector or curvilinear transducers are better. Higher-frequency probes provide better image resolution with less acoustic penetration, whereas lower-frequency probes generate better penetration but lower image resolution [14].

Acoustic windows

Appropriate acoustic windows primarily depend on an open fontanelle. On average, the time of closure of the fontanelles ranges 13–24 months for the anterior [15], 6–8 weeks for the posterior [16] and 6–18 months for the mastoid [17]. Neonatal neurosonography is typically executed through the anterior fontanelle, which is an excellent acoustic window to the supratentorial structures. Additional acoustic windows include the posterior fontanelle, which might be used to evaluate the occipital region, posterior horns of the lateral ventricles, and the cerebellum; the temporal window, which might be useful to visualize the circle of Willis and its major branches; the mastoid fontanelle, which is primarily used to visualize the cerebellum, the brainstem and the third ventricle; and the foramen magnum window, which might be used to visualize the craniocervical junction and to evaluate posterior fossa dural sinuses [3, 18–20]. Supplementary views, when present, might be taken through Burr holes, craniotomy defects, or thin areas of the parietal bones [20]. When it is deemed clinically necessary to assess the vascular structures, it may be advantageous to use spectral, color or power Doppler imaging through a fontanelle or a transcranial approach [3].

Standard imaging examination

According to the parameter developed by the American Institute of Ultrasound in Medicine (AIUM) in collaboration with the American College of Radiology (ACR), the Society for Pediatric Radiology (SPR), and the Society of Radiologists in Ultrasound (SRU) [3], the standard imaging examination of the neonate and infant includes coronal and sagittal views through the anterior fontanelle. These might be obtained by sweeping through the entire brain from anterior to posterior and with appropriate degrees of left and right transducer angulation, respectively. It is important to note that during the coronal sweep, additional right and left oblique coronal views of the brain help visualize the superolateral portions of the cortex.

An extensive list of major structures that can be visualized through both coronal and sagittal views has been outlined in the AIUM–ACR–SPR–SRU parameter [3]. The list includes the longitudinal cerebral fissure (interhemispheric fissure) and the lateral sulcus (Sylvian fissure) as well as the insula, frontal, parietal and occipital lobes; the corpus callosum, cingulate sulcus, septum pellucidum, cavum septi pellucidi and cavum vergae (if present); the periventricular white matter, ventricular system components and choroid plexus; the caudothalamic grooves, basal ganglia and thalami; the brainstem structures and mesencephalic aqueduct (aqueduct of Sylvius); the cerebellum and vermis of cerebellum; the posterior cerebellomedullary cistern (cisterna magna); and the orbits, skull base and branches of the anterior cerebral artery (pericallosal artery and callosomarginal artery) [3].

Cerebral anatomy

Improved anatomical understanding of conventional neurosonography is fundamental for enhanced diagnostic sensitivity. Several additional specific sulci, fissures and gyri, which were not listed in the AIUM–ACR–SPR–SRU parameter [3], are readily recognizable as long as a systematic approach is performed. Hence, our primary goals for this review are to introduce a systematic approach to identifying the most significant cerebral landmarks using routine US and to review all relevant major cerebral structures. We apply the body of knowledge that has been accumulated in the domains of CT and MRI to assist in the identification of these major sulci,

fissures, gyri, lobules and lobes, which have not been described in the neurosonography literature.

To further demonstrate critical cerebral anatomy landmarks on neurosonography, we selected a complete set of US images of the brain from a 3-day-old healthy term boy. Images were acquired using a broadband-array C5–8 probe, with 128 elements, frequency range 8–5 MHz, on a Philips Epiq 7G scanner (Philips Medical Systems, Best, the Netherlands). The anatomical terminology applied in this article follows the Federative International Programme for Anatomical Terminology [21–24]. Not included in the scope of this review article are the ultrasound evaluation of the skin and scalp tissues, the calvarial bones and skull base, the potential epidural and subdural spaces, the deep gray nuclei structures, the vascular structures, the ventricular system, or the posterior fossa structures. All the images displayed in this article were obtained through the anterior fontanelle.

A roadmap to identify the most common cerebral anatomical landmarks

Proper anatomical localization of central nervous system lesions and related structures is vital for clear communication. Additionally, neurologists and neurosurgeons rely on detailed anatomical descriptions to make an accurate correlation between the topography of a central nervous system lesion and clinical findings [21].

The problem of clearly identifying the brain's anatomy has been approached with a variety of methods, and several distinguishing landmarks have been described using CT and MRI [25–31]. According to the aforementioned AIUM–ACR–SPR–SRU parameter, the standard neonate and infant neurosonography examination includes coronal and sagittal views and a list of specific anatomical structures [3].

We propose the use of a systematic approach to identify the most important landmarks of the neonatal brain. This additional neurosonography acquisition would begin at the sagittal midline plane (combining modified sagittal and coronal sweeping at the same acquisition), with the corpus callosum as the starting point (Fig. 1). We have chosen to begin with the identification of the corpus callosum because this is a readily identifiable structure, and it is commonly associated with a variety of brain anomalies such as callosal dysgenesis, holoprosencephaly, Chiari II malformation, and Dandy–Walker malformation.

When scanning the brain with the fixed conventional sagittal and coronal approaches, and if a systematic approach is not implemented, the recognition of specific sulci and gyri at the convexities or at a far lateral scanning is challenging because of the lack of an accurate reference point.

Some structures are better seen in the sagittal view and vice versa. Structures that are better identified (though not exclusively) in the sagittal plane are as follows: the corpus callosum, sulcus of corpus callosum, cingulate gyrus, cingulate sulcus, marginal branch, parieto-occipital sulcus, precuneus, cuneus, calcarine sulcus and lingual gyrus. In the coronal plane, structures that are better recognized (again, not exclusively) are as follows: the central sulcus; the precentral sulcus and gyrus; the superior, medial and inferior frontal gyri; the superior and inferior frontal sulci; the orbitofrontal region; the superior, medial and inferior temporal gyri; the superior and inferior temporal sulci; the transverse temporal gyrus; the medial temporal lobe structures; the base of the temporal lobe; the lateral sulcus; the postcentral sulcus; the gyrus; the intraparietal sulcus; the superior and inferior parietal lobules; the superior, middle and inferior orbital gyri; and the superior and inferior sulci. In both the sagittal and coronal planes the following structures are clearly visible: the corpus callosum, the lateral sulcus, the sulcus of corpus callosum, the cingulate gyri, the circulate sulcus and the marginal branch. All cerebral structures mentioned in this review are seen in both cerebral hemispheres, with the exception of the corpus callosum.

Initiating the acquisition with a midline sagittal view (Fig. 2) allows for the identification of the corpus callosum, sulcus of corpus callosum, cingulate gyrus, cingulate sulcus and marginal branch. To evaluate the lateral sulcus, the insula, the inferior frontal gyri and the lateral surface of the temporal lobes, sweep the probe laterally to the left and right (Fig. 2). Return to the midline sagittal view (Fig. 2). The next step would be to tilt the probe slightly posteriorly, centering the US beam into the marginal branch of the cingulate sulcus (Fig. 2). To examine the lateral surface of the cerebral hemisphere, rotate the probe 90° at the convexity, centering the US beam into the marginal branch of the cingulate sulcus (Fig. 2). Through a coronal view, sweep anteriorly toward the orbits (Fig. 2). This enables identification of the central sulcus; precentral sulcus and gyrus; the superior, medial and inferior frontal gyri; the superior and inferior frontal sulci; the orbitofrontal region; the superior, medial and inferior temporal gyri; the superior and inferior temporal sulci; the transverse temporal gyrus; the medial temporal lobe; the base of the temporal lobe; and the lateral sulcus.

Again, through a coronal approach at the level of the marginal branch of the cingulate sulcus, sweep the probe posteriorly toward the occipital pole (Fig. 2). This approach reveals the postcentral sulcus, and gyrus, the intraparietal sulcus, and the superior and inferior parietal lobules. Returning to the sagittal midline approach, centered at the marginal sulcus (Fig. 2), the remainder of the midline parietal and occipital structures can be detected, namely the parieto-occipital sulcus, precuneus and cuneus; additionally, the calcarine sulcus and lingual gyrus can be identified. Last, through lateral oblique sweeps to the right and the left, the lateral surface of the occipital lobes can be examined and the superior, middle and

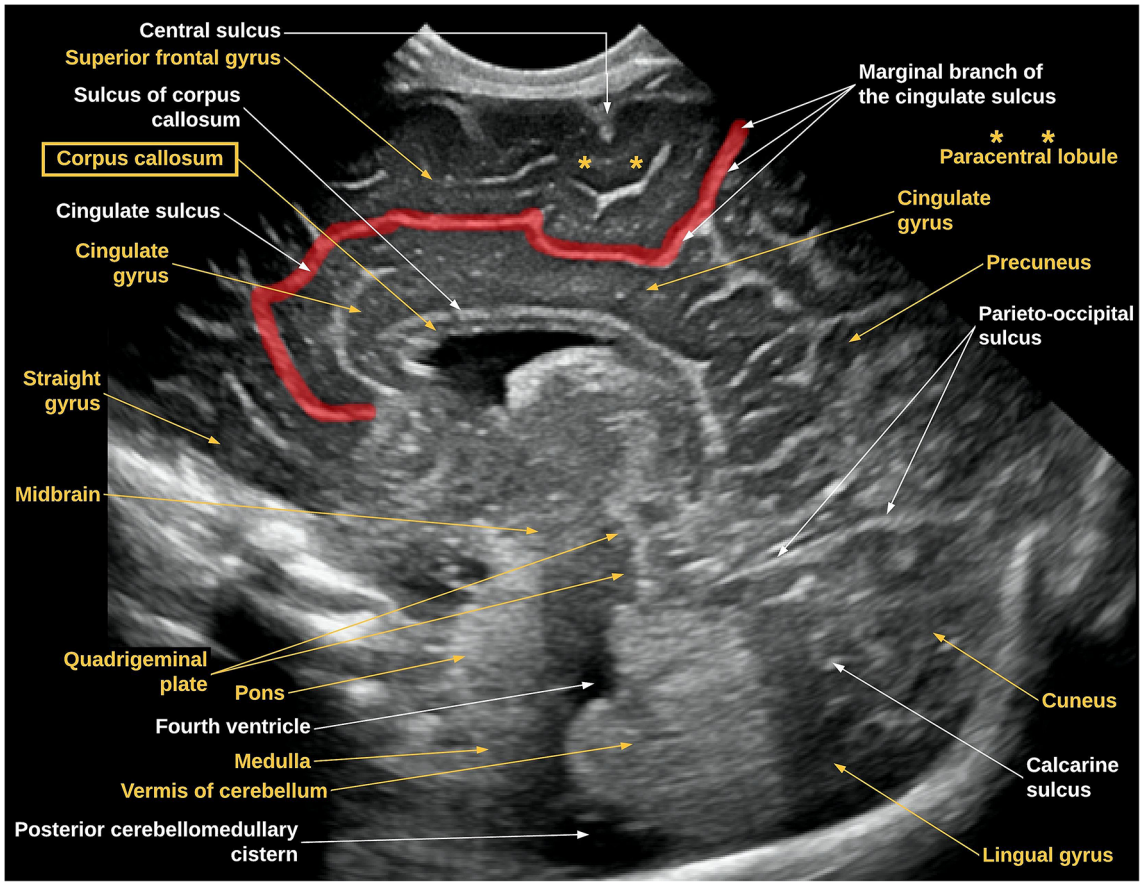

Fig. 1 Neurosonography image in the sagittal plane of a 3-day-old healthy term boy obtained through the midline with the probe placed at the anterior fontanelle. Several midline structures are highlighted. The corpus callosum can be entirely delineated, and therefore is a reliable hallmark that can be used as a starting point to localize the remainder of the midline structures. Once the corpus callosum is found, the remaining midline structures from the frontal, parietal and occipital lobes can be promptly identified. In this view, the brainstem and vermis of cerebellum are also easily depicted. The paracentral lobule is composed of the gyri located around the central sulcus (*asterisks*)

inferior orbital gyri and superior and inferior sulci can be detected on both sides (Fig. 2).

For the purpose of clarity and consistency (in the following sections), the sulci and fissures in the figures have been labeled in white and the gyri in yellow. The marginal branch of the cingulate sulcus has been highlighted in red in some figures.

Normal echotexture of brain structures

Thorough knowledge of the normal echotexture of all intracranial structures is of paramount importance in detecting normal variants and pathological conditions. Here we review the commonly understood anatomy of the neonatal brain. In the following section, we will discuss how developments in neurosonography expand our shared knowledge. The first intracranial layer visible at US is the arachnoid membrane, which with its echoes of high amplitude (hyperechoic) can be seen almost immediately in neonatal neurosonography (Fig. 3) [32]. The pia mater (in the outermost surface of the brain and spinal cord) is seen as a thin, continuous and well-defined hyperechoic layer immediately covering the gray matter (Fig. 3). The outer pial surface has a thinner echo compared to the sulcal pial surface. In the healthy neonatal brain, the juxtaposition of two pial surfaces along the sulci causes the pia mater in the sulci to appear thicker than it appears on the brain surface (Fig. 3) [32]. Gray matter and white matter have different levels of echogenicity. In the full-term, healthy neonatal brain, white matter shows higher echoes than does gray matter (Fig. 3) [33, 34]. The absence of these normal layers of distinct echogenicities might indicate pathology [19, 35].

Because of an anisotropic effect of scanning, there could be linear areas of periventricular increased echogenicity, particularly along the trigones of the lateral ventricles [36, 37]. These areas of increased echogenicity, which are called periventricular halo, flare or blush, are imaging pitfalls that can mimic periventricular leukomalacia or parenchymal hemorrhage (Fig. 4) [4, 36–38]. From the anterior fontanelle approach, the US beam passes through the white matter tracts and blood vessels of the superior and posterior trigonal regions

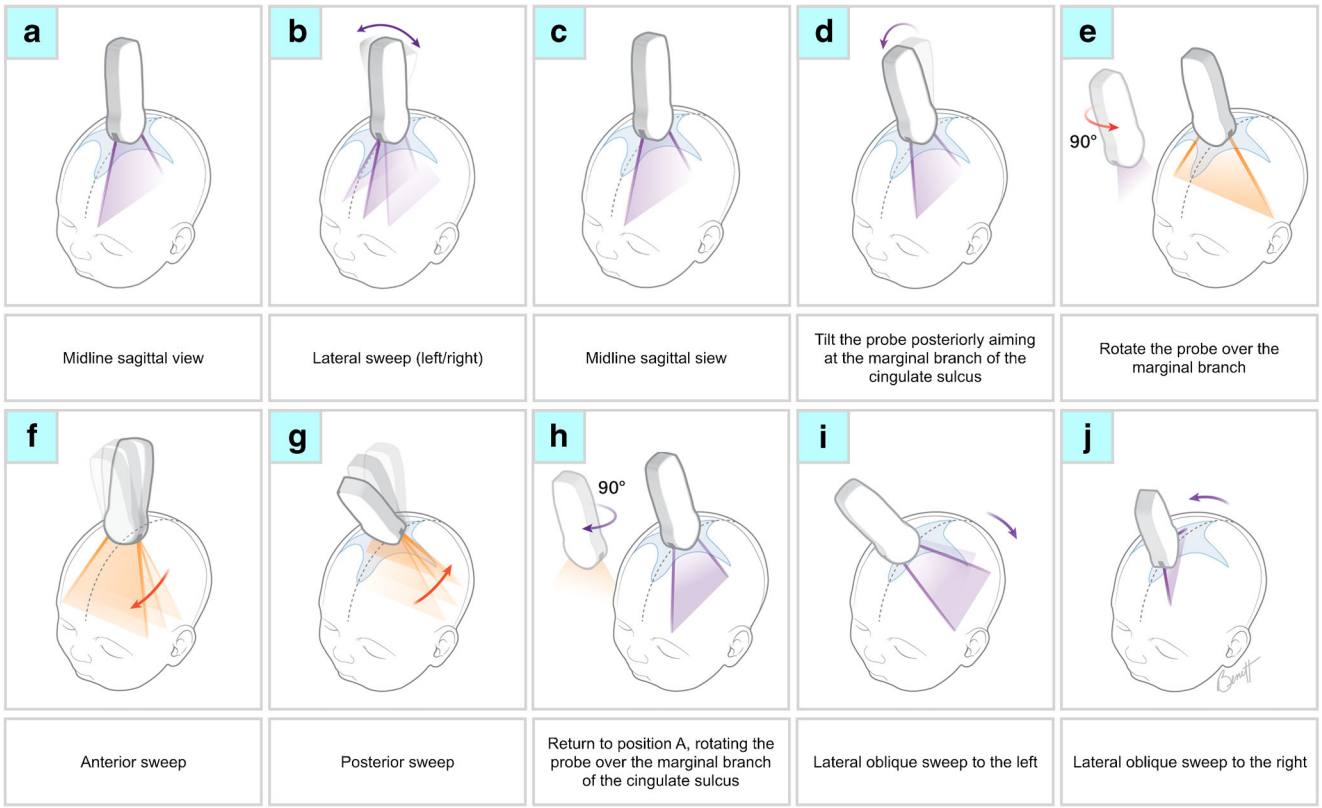

Fig. 2 Diagram shows systematic approach for the anatomy of the neonatal cerebrum, with the corpus callosum as the proposed starting point to identify the anatomy of the neonatal brain

almost perpendicularly, creating multiple sonographic interfaces. These interfaces generate a relatively homogeneous, flame-shaped hyperechogenicity with ill-defined margins in the peritrigonal area. However, the

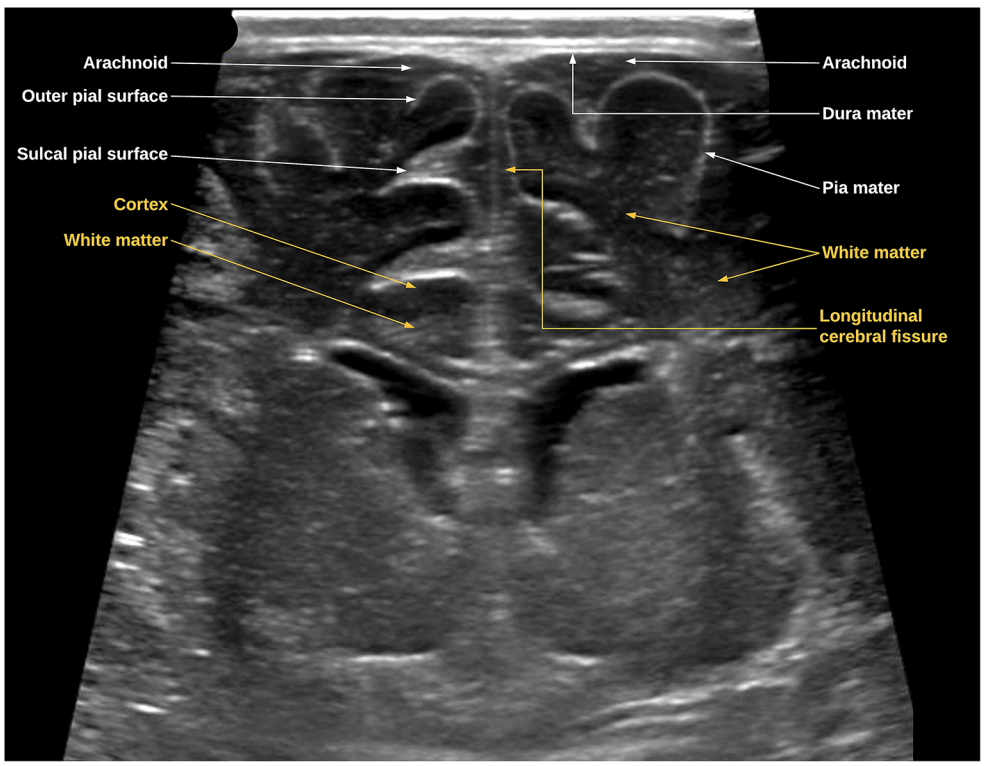

Fig. 3 Coronal US image in a 3-day-old boy of the arachnoid, which is one of the three meninges that protect and cover the brain and spinal cord. This is promptly seen in neonatal neurosonography as a hyperechoic mesh intertwined with hypoechoic foci representing cerebrospinal fluid, between the dura and the pia mater. The pia mater in the outermost surface of the brain and cord is seen as a thin, continuous and well-defined hyperechoic layer immediately covering the gray matter (cortex). The outer pial surface normally has a thinner echo compared to the sulcal pial surface. Gray matter and white matter demonstrate different echogenicities. In the full-term, healthy neonatal brain, white matter shows higher echoes when compared with gray matter

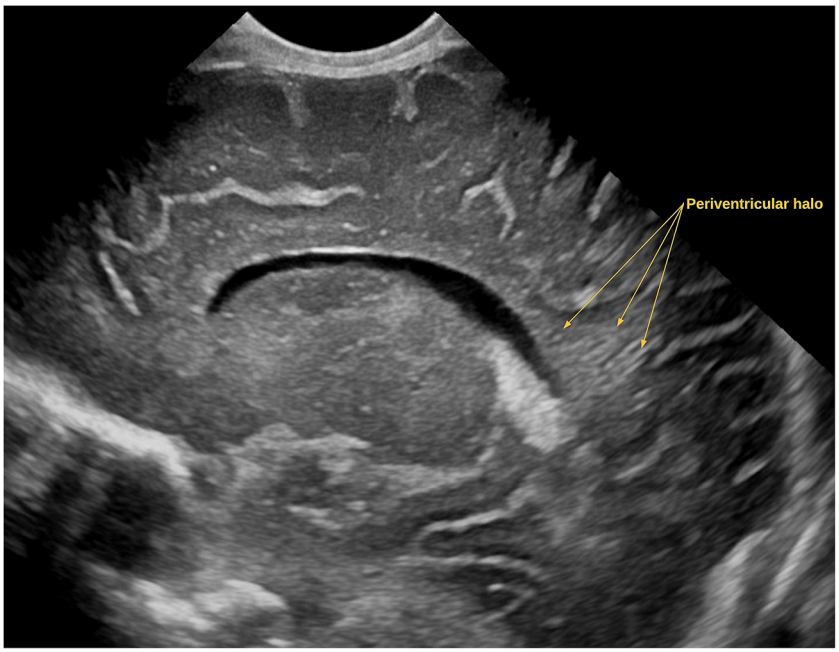

Fig. 4 Sagittal image of a 3-day-old boy. The periventricular halo represents a homogeneous ill-defined flame-shaped hyperechoic area in the periventricular white matter along the trigones of the lateral ventricles. This is a pitfall finding that can mimic periventricular leukomalacia or parenchymal hemorrhage

periventricular halo is not so evident through the posterior fontanelle, in which the US beam is oriented more parallel to the fibers [39, 40].

The structures that contain cerebrospinal fluid show as homogeneous with very low echo amplitude (anechoic), particularly in the ventricular system. The choroid plexus shows higher echogenicity than other structures in the brain, likely because of the multiple interfaces of liquid and solid structures in the villus crypts and to its increased vascularity [41]. The cerebral vasculature is readily depicted in neurosonography. On real-time US, the superficial vessels are recognizable within fissures and cisterns as pulsating tubular structures with high echo walls and low echo lumen. Color Doppler imaging improves the detection of the brain vessels, allowing for flow direction demonstration and blood velocity calculation [32].

Corpus callosum

The corpus callosum is the largest telencephalic white matter commissure (Fig. 4) [42]. This curved and elongated midline structure (in the sagittal plane) is responsible for interhemispheric communication among the sensory, motor and higher-order brain regions [43–47].

The corpus callosum is best seen in the sagittal plane, which is considered the gold standard plane to diagnose callosum abnormalities [44, 48]. Recognition of the corpus callosum facilitates the identification of several other midline structures (Fig. 4). Immediately above the corpus callosum lies the sulcus of corpus callosum and cingulate gyrus.

Sulcus of corpus callosum, cingulate gyrus and cingulate sulcus

The cingulate gyrus can be identified immediately above the corpus callosum (Fig. 4). The sulcus between the corpus callosum and cingulate gyrus is called the sulcus of corpus callosum. The cingulate gyrus is part of the limbic system, along with the hippocampus, amygdaloid body, hypothalamus and basal forebrain, as well as the parahippocampal, entorhinal, orbitofrontal, anterior cingulate and insular cortices. The limbic system is involved in emotion, memory and homeostatic processes. The cingulate gyrus is involved in many crucial neural circuits, such as those with reward centers, amygdaloid body, lateral prefrontal cortex, parietal cortex, motor areas, spinal cord, hippocampus and limbic regions [49]. The cingulate sulcus, a principal midline landmark, can be subsequently recognized as the sulcus above the cingulate gyrus. Most of the limbic structures can be identified in neurosonography.

The cingulate sulcus lies superior to the cingulate gyrus in both sagittal and coronal planes (Fig. 4). The cingulate sulcus originates in the subcallosal area with a curved anteroposterior course in the sagittal plane, paralleling the components of the corpus callosum. The cingulate sulcus can be entirely delineated in the sagittal plane, running from below the rostrum of the corpus callosum to the parietal vertex. The sulcus is the longest on the

medial surface of each hemisphere (in the sagittal plane), typically with a mildly wavy configuration. The sulcus spreads out anteroposterior from the frontal to the parietal lobes. An additional pivotal midline landmark to be identified is the marginal sulcus of the cingulate sulcus.

Parieto-occipital sulcus and precuneus and cuneus

The parieto-occipital sulcus is a deep sulcus in the medial surface of each hemisphere that separates the precuneus in the parietal lobe from the cuneus in the occipital lobe. The parieto-occipital sulcus is seen from the superior edge of the hemisphere to the anterior portion of the calcarine fissure (Fig. 4).

Calcarine sulcus and lingual gyrus

A prominent landmark on the medial aspect of the occipital lobe is the calcarine sulcus. The calcarine sulcus separates the cuneus (above) from the lingual gyrus (below) (Fig. 4). The lingual gyrus is a component of the primary visual cortex, along with the cuneus. The lingual gyrus is associated with color perception and is involved in the visual processing of the upper quadrant of the opposite visual field [50].

Marginal branch of the cingulate sulcus

The marginal branch is the caudal-most component of the cingulate sulcus [30]. In the sagittal plane, the marginal branch has a vertical course, separating the paracentral lobule (pre- and postcentral gyri) from the precuneus (Fig. 4). In the coronal plane, which is acquired with oblique angulation on US imaging, the marginal branch has a horizontal course, perpendicular to the US beam. The marginal branch (Fig. 5) is of paramount importance for locating the central sulcus on cross-sectional imaging [30], which may present several patterns, including a "bracket," as described by Naidich et al. [25]. Immediately anterior to the marginal branch lies the postcentral gyrus.

Central sulcus

The central sulcus (Fig. 5), along with the lateral sulcus and intraparietal sulcus, is one of the most relevant sulcal anatomical landmarks in the cerebral convexities. The central sulcus not only separates the

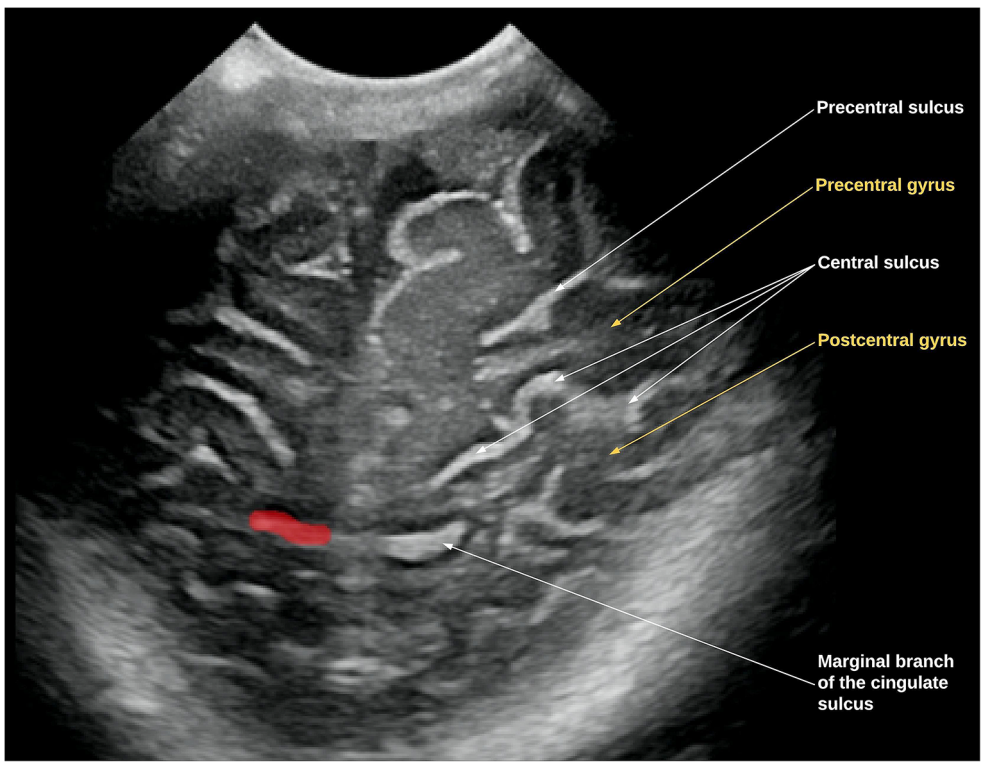

Fig. 5 Neurosonography image of a 3-day-old boy in the coronal plane obtained at the vertex with the probe placed at the anterior fontanelle. The postcentral gyrus and the central sulcus lie immediately anterior to the marginal branch of the cingulate sulcus (*red*). The marginal branch is a useful anatomical landmark to localize the central sulcus and, therefore, the remainder of the cortical structures

frontal from the parietal lobe but also is the structure that divides the primary motor cortex anteriorly (precentral gyrus) from the primary somatosensory cortex posteriorly (postcentral gyrus) (Fig. 5) [25]. Correct localization of the central sulcus is crucial for the identification of further superficial structures. After the central sulcus has been characterized, two probe directions can be taken, one anterior toward the frontal pole and one posterior toward the occipital lobe. Sweeping the probe anteriorly, the precentral sulcus and precentral gyrus can be identified.

Precentral sulcus and gyrus

In the coronal plane, the precentral sulcus is an oblique-oriented sulcus, running parallel and immediately anterior to the central sulcus (Fig. 5). The precentral and central sulci are, respectively, the anterior and posterior boundaries of the precentral gyrus (Fig. 5), which represents the primary motor area. The representation of each body part in the motor cortex is proportional to the precision of movement control. Therefore, the motor areas for the hands, face and tongue are disproportionately large. A useful landmark for identifying the motor cortex is the motor hand area, which resembles an inverted capital omega (Fig. 6) [51]. Sweeping farther anteriorly, the next structures to be identified are the superior, middle and inferior frontal gyri and the superior frontal and inferior frontal sulci.

Superior, middle and inferior frontal gyri and superior and inferior frontal sulci

Three obliquely oriented gyri lie anterior to the precentral sulcus, the superior frontal, middle frontal, and inferior frontal gyri (Fig. 7). Two sulci separate those gyri: the superior frontal and inferior frontal sulci. The superior frontal sulcus is the lateral boundary of the superior frontal gyrus (Fig. 7). The superior frontal gyrus merges with the precentral gyrus in the medial surface of the frontal lobe near the convexity (Fig. 7). Moreover, the superior frontal gyrus is separated from the cingulate gyrus by the cingulate sulcus (Fig. 7) [51]. The posterior third of the superior frontal gyrus represents the supplementary motor area, immediately anterior to the precentral gyrus. This supplementary motor area is responsible for the planning of complex movements of contralateral extremities and also contributes to ipsilateral motor planning [52].

The middle frontal gyrus is a broad gyrus located between the superior frontal sulcus and inferior frontal sulcus, anterior to the precentral sulcus and gyrus (Fig.

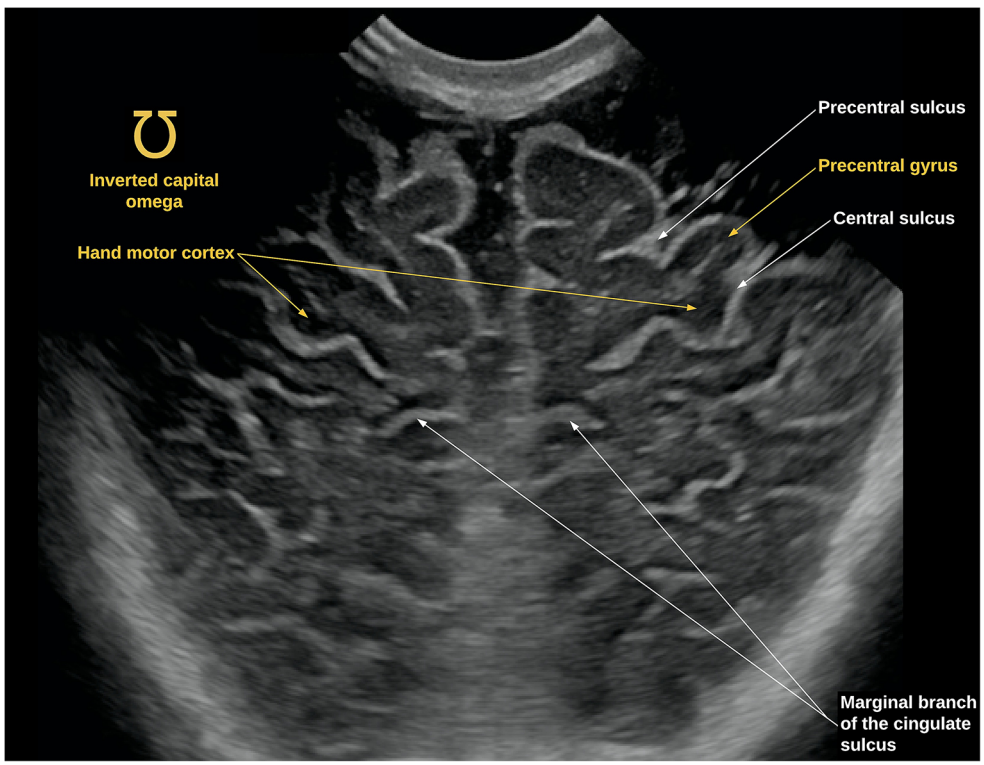

Fig. 6 Neurosonography image of a 3-day-old boy in the coronal plane obtained at the vertex with the probe placed at the anterior fontanelle. Note a focal precentral gyrus posterior bulge, which represents the hand motor area. This posterior bulge generates a useful sign to identify the hand motor cortex, known as the inverted capital omega sign

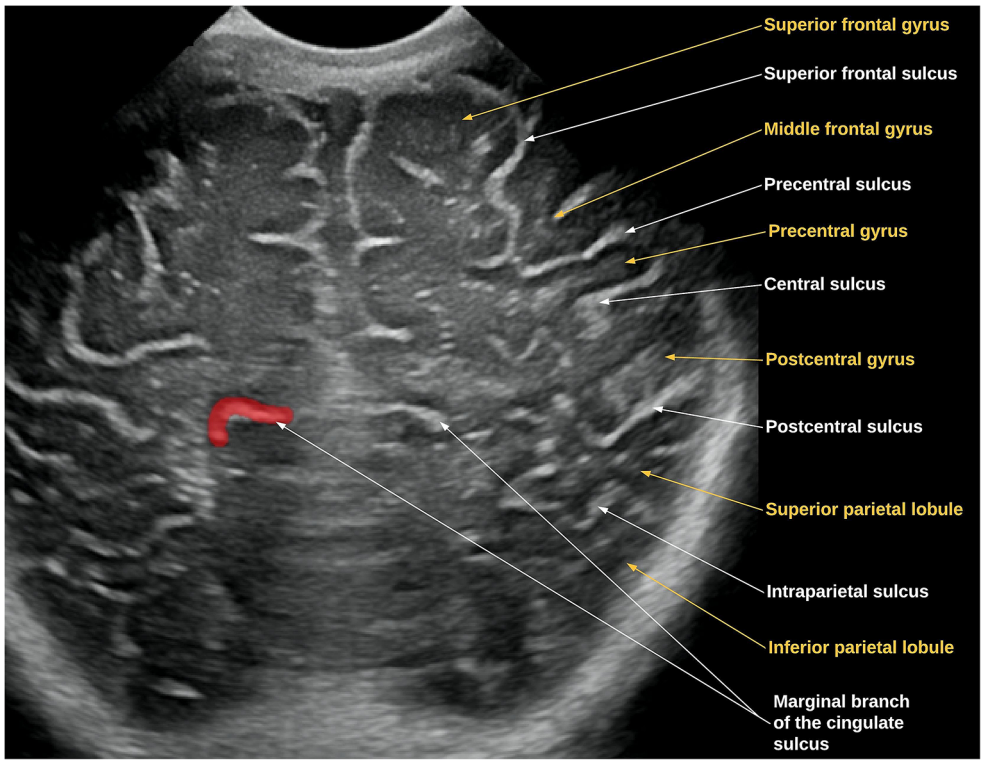

Fig. 7 Neurosonography image of a 3-day-old boy in the coronal plane obtained anterior to Fig. 6, with the probe placed at the anterior fontanelle. The central sulcus is located anteriorly in relation to the marginal branch. Anterior to the central sulcus lie the precentral gyrus, precentral sulcus, middle frontal sulcus and middle frontal gyrus (the inferior frontal sulcus and gyrus are better seen in Figs. 8 and 9). The superior frontal sulcus is the lateral boundary of the superior frontal gyrus. The superior frontal gyrus merges with the precentral gyrus in the lateral surface of the frontal lobe near the convexity

7). The middle frontal gyrus has a complex configuration with anterior and posterior parts. The anterior part can be further divided into ventral and dorsal components. The posterior part is even more sub-segmented into multiple small gyri. The middle frontal gyrus represents at least one-third of the frontal lobe and is responsible for higher cognitive functions, such as reorienting attention [53].

The inferior frontal gyrus represents a significant component of the prefrontal cortex lying between the inferior

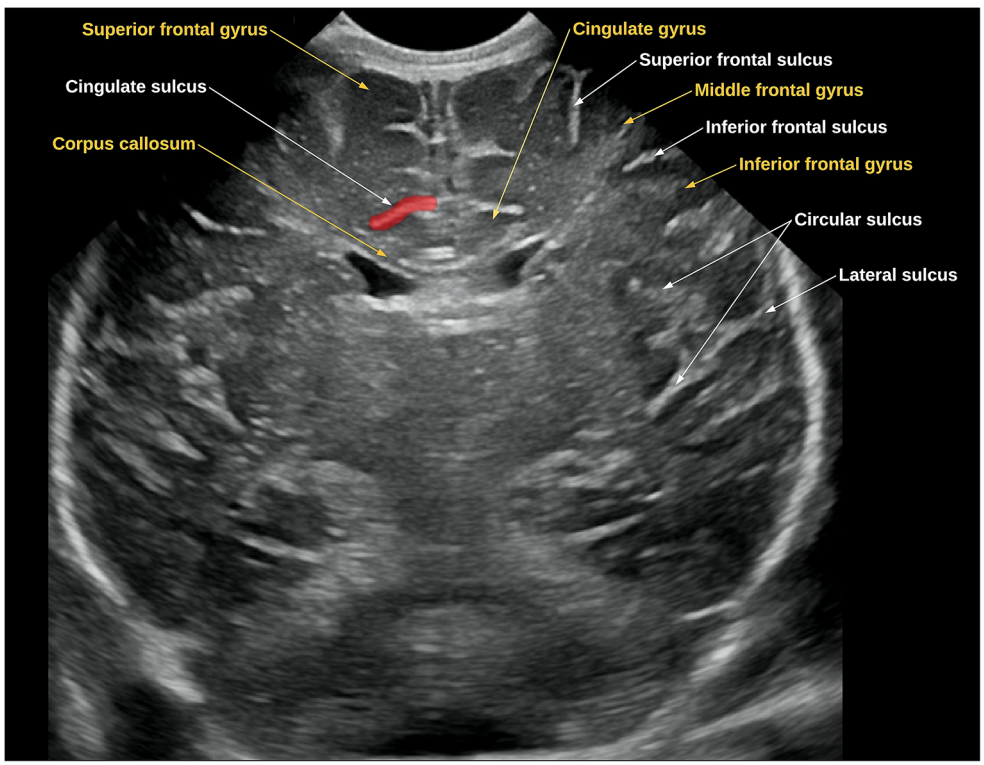

Fig. 8 Neurosonography image of a 3-day-old boy in the coronal plane obtained anterior to Fig. 7, with the probe placed at the anterior fontanelle. The central sulcus is not evident in this plane. From the lateral sulcus, the reader can identify the inferior frontal gyrus and sulcus, the middle frontal gyrus, and the superior frontal sulcus and gyrus. In the medial surface of the brain, the superior frontal gyrus is separated from the cingulate gyrus from the cingulate sulcus

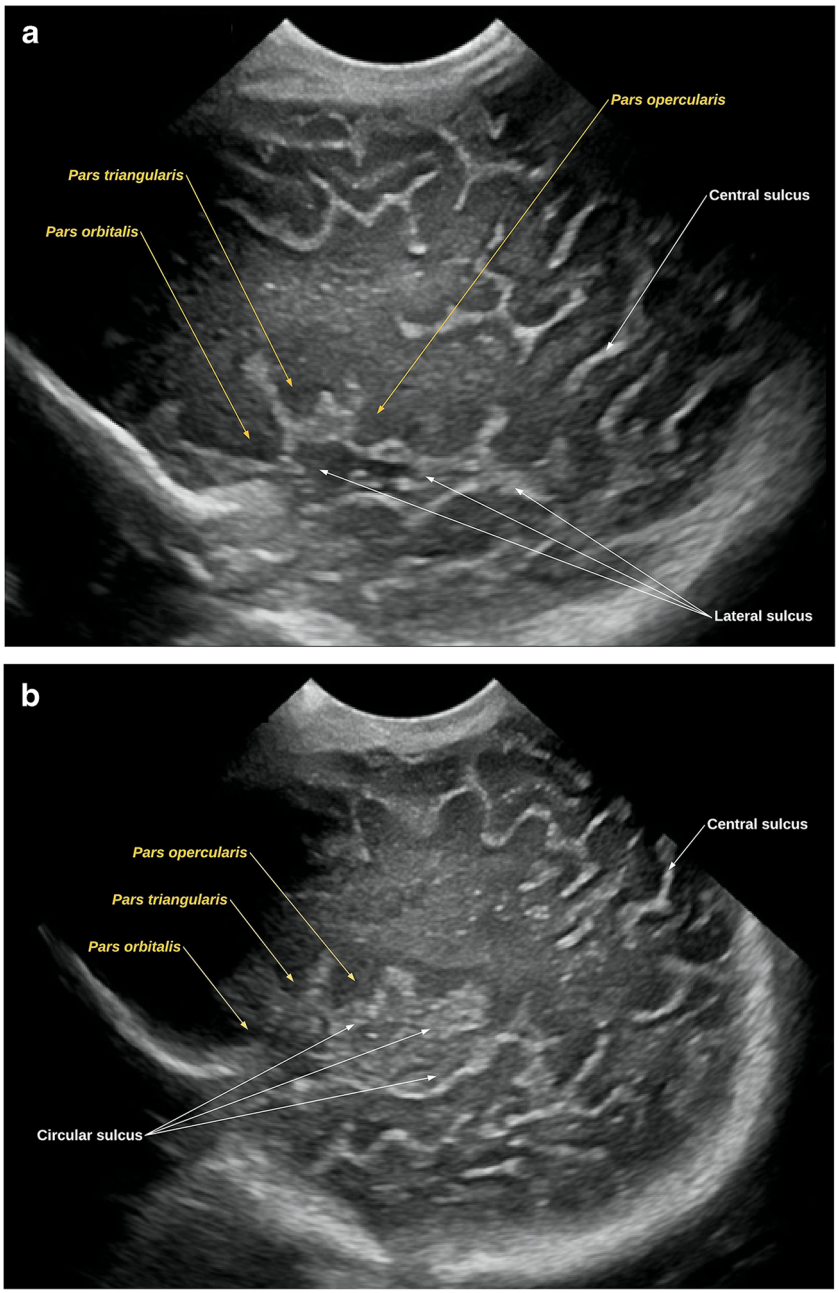

Fig. 9 Neurosonography images of a 3-day-old boy (**a** and **b**) in the sagittal oblique plane obtained slightly anterior to Fig. 8, with the probe located at the anterior fontanelle. The central sulcus is evident posteriorly in this plane. After localizing the lateral sulcus, the reader can identify the major components of the inferior frontal gyrus. From posterior to anterior, the inferior frontal gyrus can be divided into three parts: the pars opercularis, the pars triangularis, and pars orbitalis

frontal sulcus and lateral sulcus (Figs. 8 and 9) [54]. From posterior to anterior, the inferior frontal gyrus can be divided into three parts: the pars opercularis, the pars triangularis and pars orbitalis (Fig. 9). The borders of the pars opercularis are the lateral sulcus inferiorly, the precentral sulcus posteriorly, and the anterior ascending ramus of the lateral sulcus anteriorly. The pars triangularis is located between the anterior ascending and horizontal rami of the lateral sulcus anteriorly and posteriorly, respectively (Fig. 9). The pars orbitalis lies anterior to the horizontal ramus of the lateral sulcus (Fig. 9) [54]. The inferior frontal gyrus is responsible for various highly complex functions, including language processing, comprehension and production [55]. Sweeping anteriorly toward the frontal poles, the next structures to be identified are the orbitofrontal region structures.

Orbitofrontal region

The orbitofrontal region is a flat or slightly anteriorly concave area that surrounds the floor of the anterior skull base, superior to the roof of the orbit (Fig. 10)

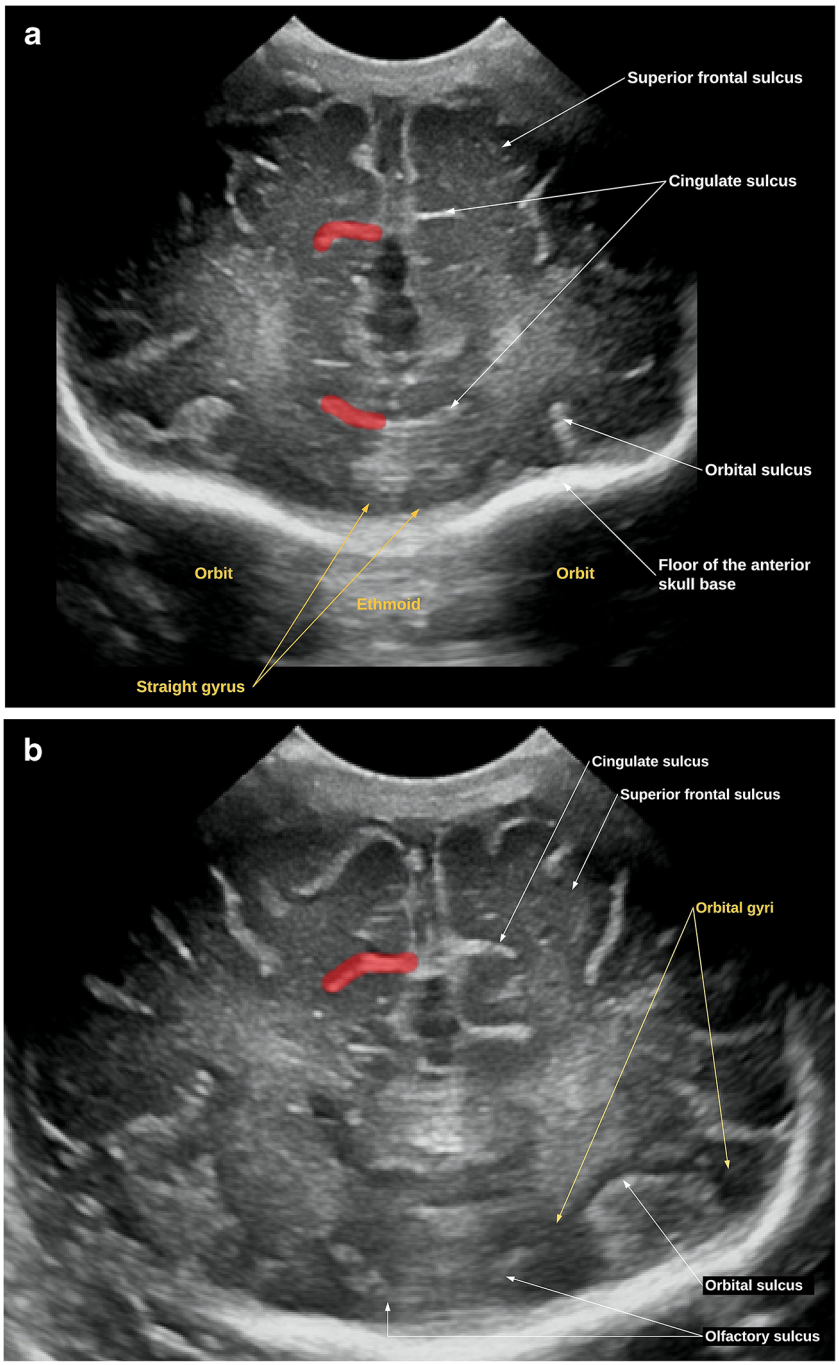

Fig. 10 Neurosonography images of a 3-day-old boy in the coronal plane obtained anterior to Fig. 9, with the probe placed at the anterior fontanelle aiming at the eye globes. Neither the central sulcus nor the lateral sulcus is evident in this plane. **a, b** After localizing the anterior skull base, the reader can detect the eye globe and ethmoid labyrinth (**a**) and the most relevant structures of the orbitofrontal region. The main structures in this region are the olfactory and orbital sulci, the straight gyrus and the orbital gyri (**a** and **b**)

[21]. The straight gyrus is located at the midline, superior to the ethmoid labyrinth and cribriform plate. The ethmoid bone is represented on US by the increased focus of echogenicity between the orbits, immediately below the anterior skull base (Fig. 10). The olfactory groove can occasionally be visualized. The olfactory sulcus (Fig. 10) is located a few millimeters from the midline, medial to the straight gyrus. The orbital sulcus is located further laterally (Fig. 10), with a complex configuration in the coronal plane. The orbital gyrus forms the remainder of the lateral orbitofrontal region, which is subdivided into anterior, posterior medial and lateral parts by the orbital sulcus [21].

Superior, middle and inferior temporal gyri and superior and inferior temporal sulci

The lateral sulcus is readily visible on the lateral surface of each cerebral hemisphere. It is absolutely necessary to

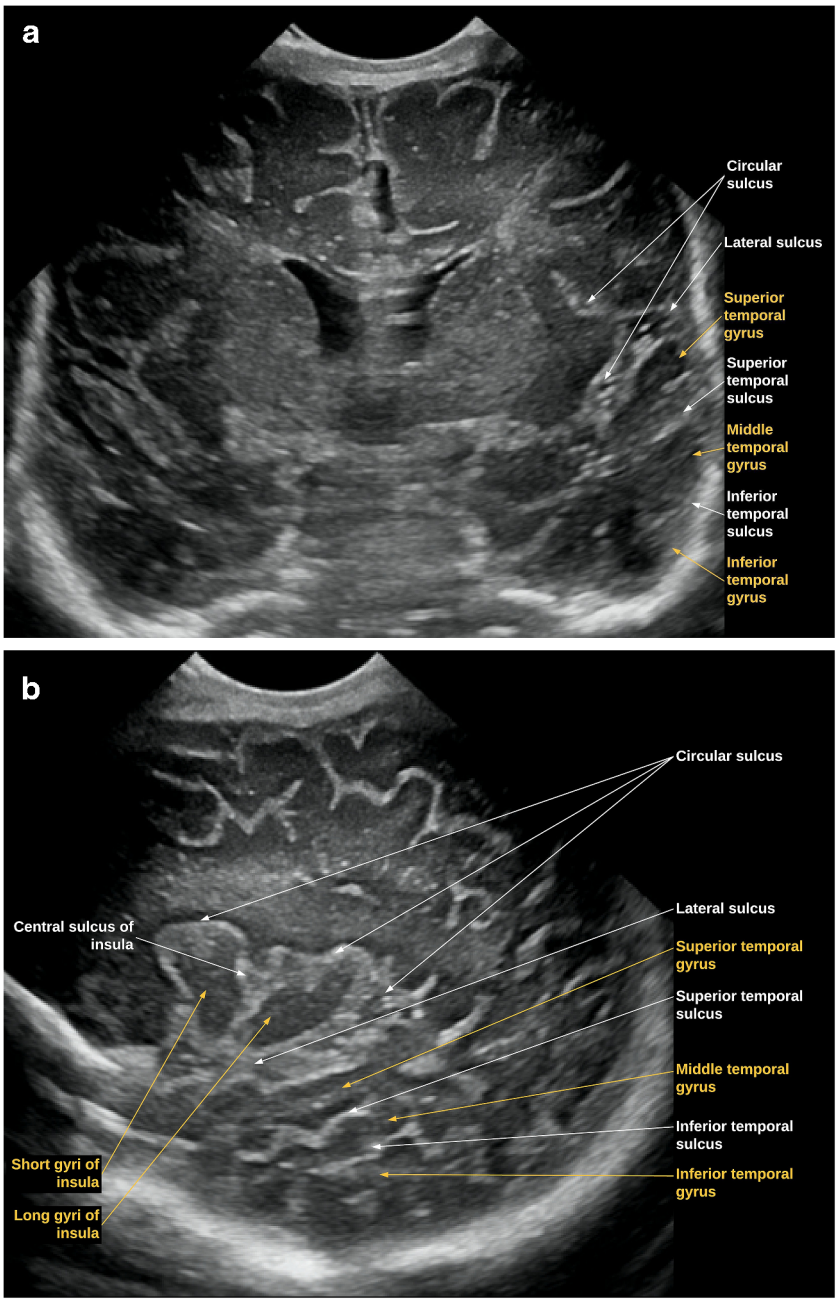

Fig. 11 Neurosonography images of a 3-day-old boy in the coronal plane (**a**) and sagittal plane (far lateral) (**b**) obtained posterior to Fig. 10, with the probe placed at the anterior fontanelle aiming at the basal ganglia and lateral sulcus. After localizing the lateral sulcus, the reader can detect the frontal lobe superiorly and the temporal lobe inferiorly. The main structures in this region are the superior, middle and inferior temporal sulci and the superior and middle temporal gyri

precisely delineate the lateral sulcus. On fetal US, an increased angulation of the lateral sulcus may be a strong early indicator for cortical development malformation [56]. The lateral sulcus is frequently abnormal in cases of perisylvian polymicrogyria, which assumes an abnormal course, extension and orientation, appearing extended and oriented posterosuperiorly [57]. Various other disorders of cortical development malformation can occur with abnormal lateral sulci, such as lissencephaly, hemimegalencephaly and schizencephaly [57].

The lateral sulcus separates the temporal lobe from the frontal and parietal lobes. There are two sulci on the lateral surface of the temporal lobe, the superior temporal and inferior temporal sulci (Fig. 11). These sulci delineate the superior temporal, middle temporal and inferior temporal gyri (Fig. 11) [58].

Both the insula and the operculum can be depicted with neurosonography, described later. The insula is surrounded by a deep, circular sulcus called the circular sulcus of insula. It is contiguous with the lateral sulcus, which separates it from the operculum [59].

The *operculum* (from the Latin "little lid") consists of the cortical areas covering the adjacent insula and its surrounding

circular sulcus. The operculum is divided into three main segments: the frontal operculum, the parietal operculum and the temporal operculum. The frontal operculum contains the pars triangularis and opercularis of the inferior frontal gyrus, along with the Broca area (in the dominant hemisphere), which is essential for language function [60]. The parietal operculum lies between the inferior portion of the postcentral gyrus and the posterior rami of the lateral fissure. The temporal operculum lies inferior to the lateral fissure and is formed by the superior temporal and transverse temporal gyri.

The insula (the Latin name for island), which lies below the opercula and is surrounded by the circular gyrus, is considered a separate lobe of the human brain. The insula is a complex structure involved in multiple crucial functions for human cognition and behavior, from sensorimotor, pain and socio-emotional processes to high-level attention and decision-making [61, 62]. The central sulcus of insula divides it into an anterior and a posterior part. The anterior part includes three short gyri and the posterior part two long gyri (Fig. 11) [61, 62].

Transverse temporal gyrus

In the depth of the lateral sulcus and along the superior temporal gyrus, the transverse temporal gyrus (gyrus of Heschel), can be identified as a doubled obliquely oriented cortical ridge (Fig. 12). Portions of the primary auditory cortex are located in the transverse temporal gyrus [58].

Medial temporal lobe

The medial temporal lobe contains the amygdaloid body, hippocampus, parahippocampal gyrus, subiculum, the dentate gyrus, and associated white matter, notably the fimbria of hippocampus, whose fibers continue into the fornix (Fig. 13). The subiculum, dentate gyrus, fimbria and fornix are not readily distinguishable structures on conventional neurosonography. The hippocampus is an infolded gyrus that bulges into the temporal horn of the lateral ventricle (Fig. 13). The choroid fissure (Fig. 13), alongside the fimbria of the hippocampus, separates the temporal lobe from the optic tract, hypothalamus and midbrain. The amygdaloid body (Fig. 14) comprises several nuclei on the medial aspect of the temporal lobe, mostly anterior to the hippocampus and indenting the tip of the temporal horn [58].

Base of the temporal lobe

In the base of the temporal lobe, the occipitotemporal sulcus separates the medial border of the inferior temporal gyrus from the lateral border of the fusiform or medial occipitotemporal gyrus (Fig. 13). The collateral sulcus lies medial to the fusiform gyrus and lateral to the parahippocampal gyrus (Fig. 13). The parahippocampal gyrus forms the medial border of the inferior surface of the temporal lobe (Fig. 13). At its

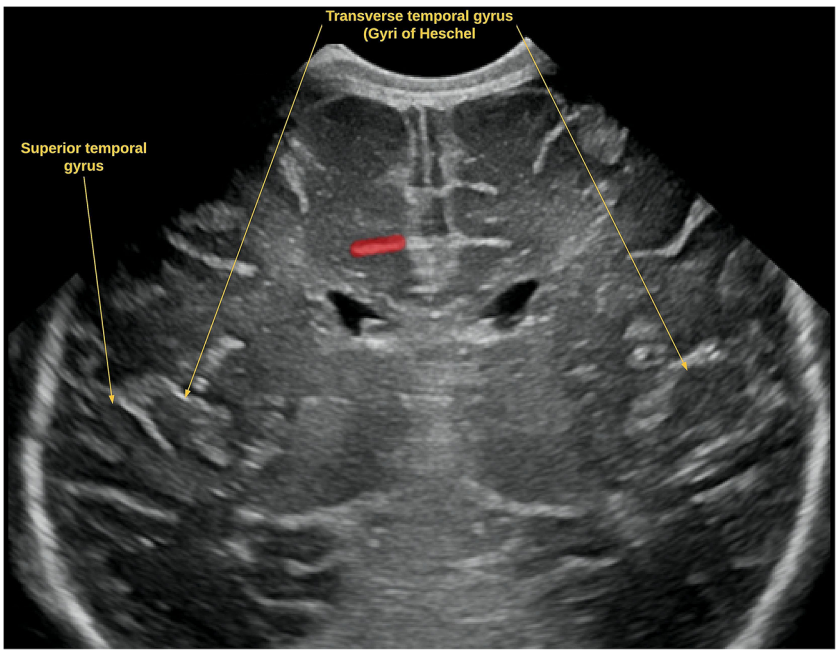

Fig. 12 Neurosonography image of a 3-day-old boy in the coronal plane obtained slightly posterior to Fig. 11, with the probe placed at the anterior fontanelle aiming at the thalamus, emphasizing the transverse temporal gyrus (gyrus of Heschel). Highlighted in red is the cingulate sulcus (right cerebral hemisphere)

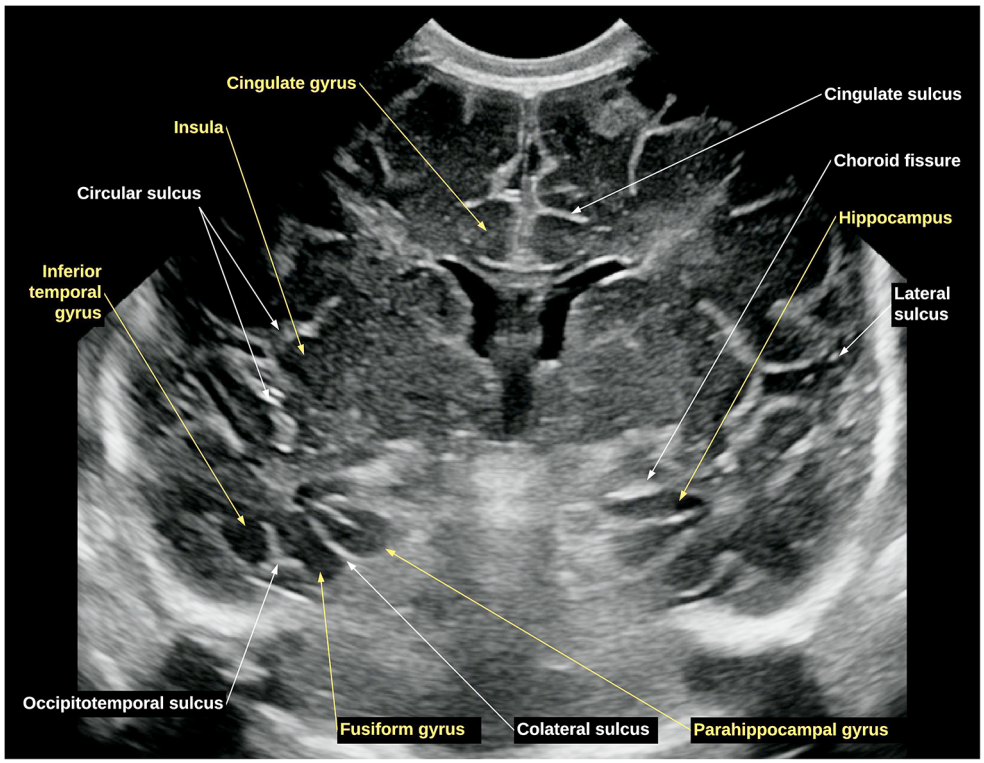

Fig. 13 Neurosonography image of a 3-day-old boy in the coronal plane obtained slightly anterior to Fig. 12, with the probe placed at the anterior fontanelle aiming at the basal ganglia, again emphasizing the medial temporal lobe. After localizing the lateral sulcus, the reader can detect the parahippocampal gyrus, hippocampus, choroid fissure, collateral sulcus, fusiform gyrus, occipitotemporal sulcus, and temporal sulci and gyri partially

anterior end is a small projection of the medial surface, called the uncus (Fig. 14) [58].

The structures at the base of the temporal lobe are involved in multiple complex functions. The inferior temporal gyrus is involved with language and semantic memory processing, visual perception, and multimodal sensory integration [63]. The fusiform gyrus is considered a key structure for functionally specialized computations of high-level vision such as face perception,

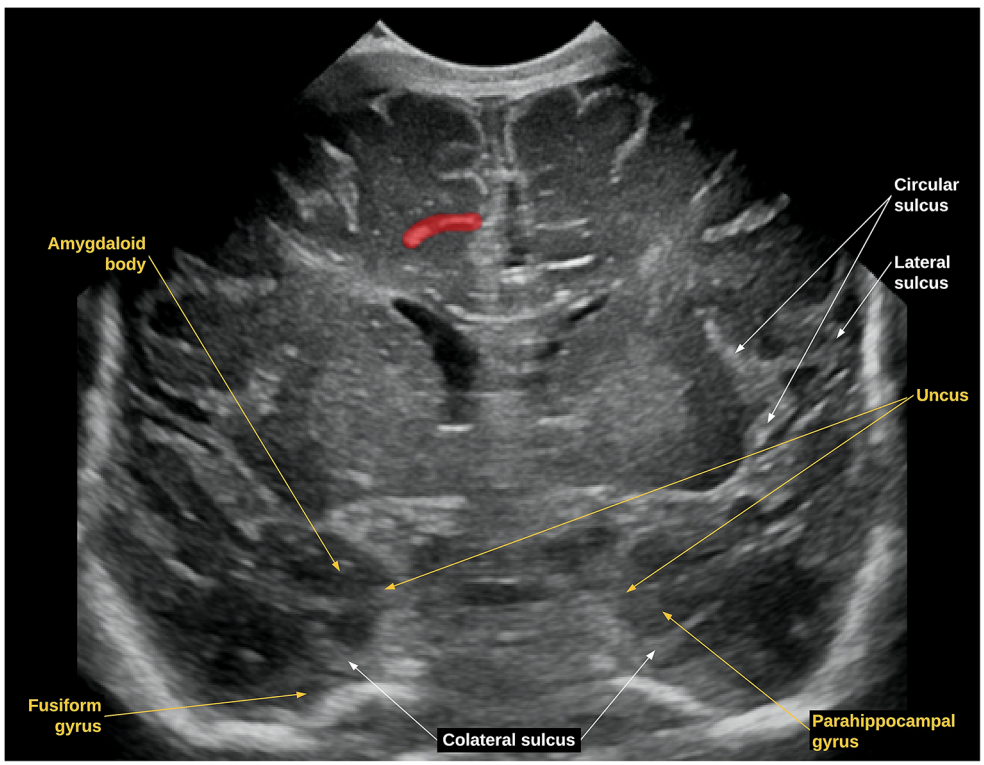

Fig. 14 Neurosonography image of a 3-day-old boy in the coronal plane obtained slightly anterior to Fig. 13, with the probe placed at the anterior fontanelle aiming at the basal ganglia, emphasizing the medial temporal lobe structures. After localizing the lateral sulcus and the uncus, the reader can detect the amygdaloid body, parahippocampal gyrus, fusiform gyrus, and temporal sulci and gyri partially

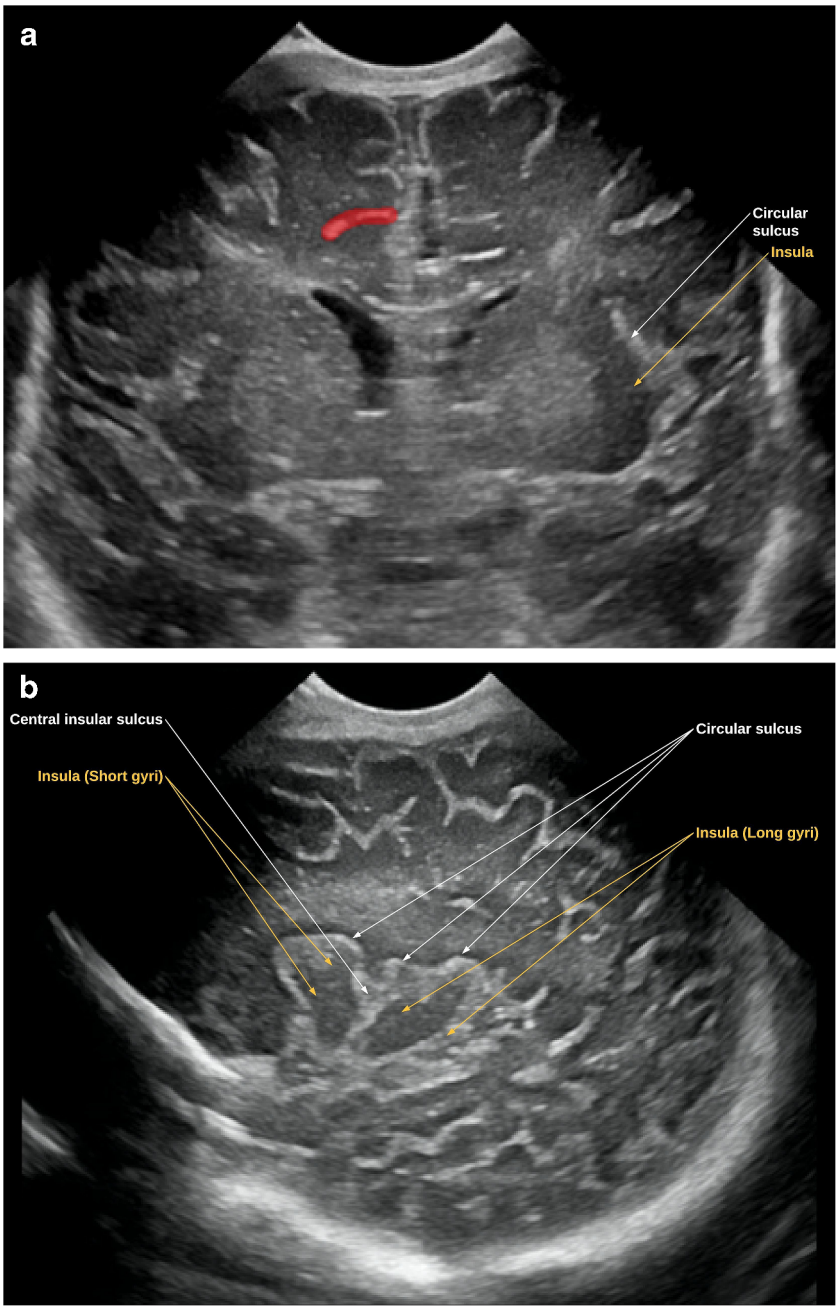

Fig. 15 Neurosonography images of a 3-day-old boy in the coronal (**a**) and sagittal (**b**) (far lateral) planes, obtained at the same level as Fig. 13, with the probe placed at the anterior fontanelle aiming at the basal ganglia, still emphasizing insula. After localizing the lateral sulcus, the reader can detect the insula, immediately medial to it, with its short and long gyri in (**b**)

object recognition, and reading [64]. The parahippocampal gyrus encompasses a large portion of the medial temporal lobe and is involved in multiple tasks such as memory formation (along with the hippocampus) and high-level visual processing [65]. The uncus, which lies at the anterior and most medial portion of the temporal lobe and adjacent to the amygdaloid body, encompasses part of the olfactory tract and therefore is associated with olfactory processing [60]. Because of its proximity to the brainstem, the uncus can compress the midbrain and the oculomotor nerve in cases of herniation over the free edge of the tentorium. Uncal herniation can occur after a rapidly expanding temporal epidural or subdural hematoma or intraparenchymal hemorrhage [66].

Lateral sulcus

The lateral sulcus is one of the most important sulci in the lateral surface of the brain (Figs. 9, 11, 13 and 14). It separates the frontal and parietal lobes superiorly from the temporal lobe anteriorly [67]. The lateral sulcus mainly contains the middle cerebral artery and its rami; it forms the cistern of the lateral

cerebral fossa (Sylvian cistern). In the depth of the lateral sulcus lies the insula with its short and long gyri (Figs. 11 and 13). The lateral sulcus extends from the anterior clinoid process to the lateral convexity. On the surface of the inferior parietal lobule, immediately posterior and adjacent to the lateral sulcus, the supramarginal gyrus can be identified (Fig. 15). Inferior and posterior to the supramarginal gyrus, the angular gyrus can be seen in continuity with the superior temporal gyrus (Fig. 15) [68].

Postcentral sulcus and gyrus

The postcentral sulcus is vertically oriented, running parallel and immediately posterior to the central sulcus, parallel to the motor cortex (Figs. 5 and 7). The central and postcentral sulci (Figs. 5, 6 and 7), are, respectively, the anterior and posterior boundaries of the postcentral gyrus, which on imaging represent the primary somatosensory cortex. The sensory strip contains an inverted map of the opposite side of the body, mirroring that of the motor strip [51].

Intraparietal sulcus and superior and inferior parietal lobules

The intraparietal sulcus is located on the lateral surface of the parietal lobe, dividing the posterior parietal region into the superior parietal and inferior parietal lobules (Fig. 7). The adjacent cortex is involved in sensorimotor functions, specifically involving movement intention formation and cognitive plans for specific types of movements [69].

Superior, middle and inferior occipital gyri and superior and inferior occipital sulci

There are three major gyri in the convexity surface of the occipital lobe: the superior occipital gyrus, middle occipital gyrus and inferior occipital gyrus, separated by the superior occipital sulcus and inferior occipital sulcus (Fig. 16). The superior occipital sulcus is usually seen as the posterior continuation of the intraparietal sulcus. The inferior occipital sulcus is usually seen as the posterior extension of the inferior temporal sulcus. The middle occipital gyrus is the largest of the three occipital gyri. The superior, middle and inferior occipital gyri are also named as the lateral occipital complex, which is associated with object recognition and face perception [70, 71].

Conclusion

Neurosonography remains an essential imaging modality in the neonatal period and infancy, particularly in the screening of germinal matrix hemorrhage, ventriculomegaly and

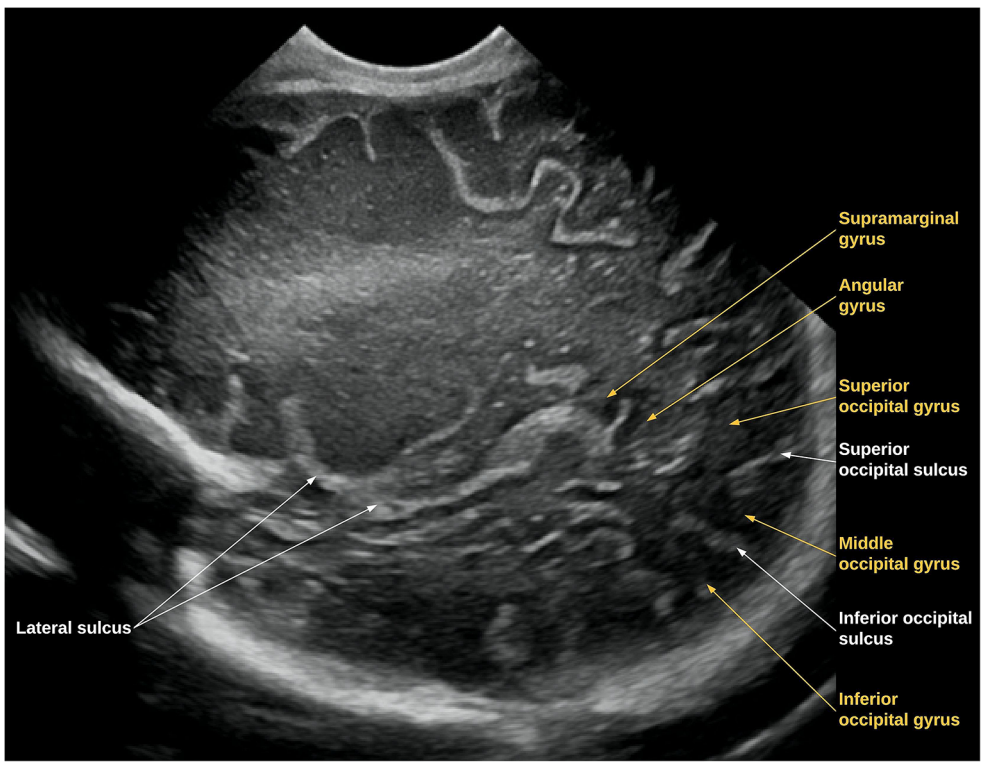

Fig. 16 Neurosonography image of a 3-day-old boy in the sagittal plane slightly posterior to Fig. 15, with the probe placed at the anterior fontanelle aiming the occipital lobe. After localizing the lateral sulcus, the reader can detect, immediately posterior to it, the supramarginal and angular gyri. In the lateral surface of the occipital lobe, the most relevant structures are the three major occipital gyri: the superior occipital gyrus, middle occipital gyrus, and inferior occipital gyrus, separated by the superior occipital sulcus and inferior occipital sulcus

periventricular leukomalacia. Neurosonography is a noninvasive and cost-effective modality that can be performed with no need for sedation and requires minimal preparation. To make the best use of these advantages, precise anatomical identification of the neonatal cerebrum structures is crucial to the localization of specific intracranial abnormalities from ischemia, hemorrhage, infection or reperfusion injury. An established roadmap for the sonographic evaluation of neonatal cerebral structures can aid in consistently identifying normal and abnormal structures. Furthermore, this standardized roadmap lends itself to being used as a framework for injury localization using advanced sonographic techniques such as elastography, high-frequency Doppler and contrast-enhanced US. Ultimately, this roadmap could be used to create an atlas of sonographic structures for automated classification of injury localization.

Acknowledgments We acknowledge Brittany C. Bennett for creating the illustrations and Lydia Sheldon for English language editing and review.

Compliance with ethical standards

Conflicts of interest None

References

1. Nagaraj N, Berwal PK, Srinivas A et al (2016) A study of neurosonogram abnormalities, clinical correlation with neurosonogram findings, and immediate outcome of high-risk neonates in neonatal intensive care unit. J Pediatr Neurosci 11:200–205
2. van Wezel-Meijler G, Steggerda SJ, Leijser LM (2010) Cranial ultrasonography in neonates: role and limitations. Semin Perinatol 34:28–38
3. American Institute of Ultrasound in Medicine (2020) AIUM practice parameter for the performance of neurosonography in neonates and infants. J Ultrasound Med 39:E57–E61
4. Gupta P, Sodhi KS, Saxena AK et al (2016) Neonatal cranial sonography: a concise review for clinicians. J Pediatr Neurosci 11:7–13
5. Llorens-Salvador R, Moreno-Flores A (2016) The ABCs of transfontanellar ultrasound and more. Radiologia 58:129–141
6. Maller VV, Cohen HL (2019) Neonatal head ultrasound: a review and update — Part 1: techniques and evaluation of the premature neonate. Ultrasound Q 35:202–211
7. Pinto A, Pinto F, Faggian A et al (2013) Sources of error in emergency ultrasonography. Crit Ultrasound J 5:S1
8. Diwakar RK, Khurana O (2018) Cranial sonography in preterm infants with short review of literature. J Pediatr Neurosci 13:141–149
9. Maalouf EF, Duggan PJ, Counsell SJ et al (2001) Comparison of findings on cranial ultrasound and magnetic resonance imaging in preterm infants. Pediatrics 107:719–727
10. Miller SP, Cozzio CC, Goldstein RB et al (2003) Comparing the diagnosis of white matter injury in premature newborns with serial MR imaging and transfontanel ultrasonography findings. AJNR Am J Neuroradiol 24:1661–1669
11. Meijler G, Steggerda SJ (2019) Limitations of cranial ultrasonography and recommendations for MRI. In: Meijler G, Steggerda SJ (eds) Neonatal cranial ultrasonography. Springer International Publishing, Cham, pp 183–194
12. Leijser LM, de Vries LS, Rutherford MA et al (2007) Cranial ultrasound in metabolic disorders presenting in the neonatal period: characteristic features and comparison with MR imaging. AJNR Am J Neuroradiol 28:1223–1231
13. Epelman M, Daneman A, Kellenberger CJ et al (2010) Neonatal encephalopathy: a prospective comparison of head US and MRI. Pediatr Radiol 40:1640–1650
14. Rumack CM, Auckland AK (2017) Neonatal and infant brain imaging. In: Rumack CM, Levine D (eds) Diagnostic ultrasound, 5th edn. Elsevier, Philadelphia, pp 1511–1572
15. D'Antoni AV, Donaldson OI, Schmidt C et al (2017) A comprehensive review of the anterior Fontanelle: embryology, anatomy, and clinical considerations. Childs Nerv Syst 33:909–914
16. Kiesler J, Ricer R (2003) The abnormal fontanel. Am Fam Physician 67:2547–2552
17. Lipsett BJ, Reddy V, Steanson K (2020) Anatomy, head and neck, fontanelles. StatPearls Publishing, Treasure Island
18. James AC (2018) Practical guide to neonatal cranial ultrasound (CrUS): basics. Paediatr Child Health 28:424–430
19. Lowe LH, Bailey Z (2011) State-of-the-art cranial sonography: Part 1, modern techniques and image interpretation. AJR Am J Roentgenol 196:1028–1033
20. Luna JA, Goldstein RB (2000) Sonographic visualization of neonatal posterior fossa abnormalities through the posterolateral fontanelle. AJR Am J Roentgenol 174:561–567
21. Destrieux C, Terrier LM, Andersson F et al (2017) A practical guide for the identification of major sulcogyral structures of the human cortex. Brain Struct Funct 222:2001–2015
22. ten Donkelaar HJ, Kachlík D, Tubbs RS (2018) An illustrated terminologia neuroanatomica. Springer International, Cham
23. Vollrath L, Fraher J, Whitmore I (2013) Terminologia embryologica: FIPAT — Federative International Programme on Anatomical Terminologies. Thieme Verlagsgruppe, Stuttgart
24. ten Donkelaar HJ, Broman J, Neumann PE et al (2017) Towards a terminologia neuroanatomica. Clin Anat 30:145–155
25. Naidich TP, Blum JT, Firestone MI (2001) The parasagittal line: an anatomic landmark for axial imaging. AJNR Am J Neuroradiol 22:885–895
26. Fesl G, Moriggl B, Schmid UD et al (2003) Inferior central sulcus: variations of anatomy and function on the example of the motor tongue area. Neuroimage 20:601–610
27. Wagner M, Jurcoane A, Hattingen E (2013) The U sign: tenth landmark to the central region on brain surface reformatted MR imaging. AJNR Am J Neuroradiol 34:323–326
28. Naidich TP, Valavanis AG, Kubik S (1995) Anatomic relationships along the low-middle convexity: Part I — normal specimens and magnetic resonance imaging. Neurosurgery 36:517–532
29. Naidich TP, Kang E, Fatterpekar GM et al (2004) The insula: anatomic study and MR imaging display at 1.5 T. AJNR Am J Neuroradiol 25:222–232
30. Sobel DF, Gallen CC, Schwartz BJ et al (1993) Locating the central sulcus: comparison of MR anatomic and magnetoencephalographic functional methods. AJNR Am J Neuroradiol 14:915–925
31. Hill VB, Cankurtaran CZ, Liu BP et al (2019) A practical review of functional MRI anatomy of the language and motor systems. AJNR Am J Neuroradiol 40:1084–1090
32. Jéquier S, Jéquier JC (1999) Sonographic nomogram of the leptomeninges (pia-glial plate) and its usefulness for evaluating bacterial meningitis in infants. AJNR Am J Neuroradiol 20:1359–1364
33. Slovis TL, Kuhns LR (1981) Real-time sonography of the brain through the anterior fontanelle. AJR Am J Roentgenol 136:277–286

34. Powell RW (1982) Real-time sonography of the brain through the anterior fontanelle. J Pediatr Surg 17:335
35. Bhat V, Bhat V (2014) Neonatal neurosonography: a pictorial essay. Indian J Radiol Imaging 24:389–400
36. DiPietro MA, Brody BA, Teele RL (1986) Peritrigonal echogenic "blush" on cranial sonography: pathologic correlates. AJR Am J Roentgenol 146:1067–1072
37. Grant EG, Schellinger D, Richardson JD et al (1983) Echogenic periventricular halo: normal sonographic finding or neonatal cerebral hemorrhage. AJR Am J Roentgenol 140:793–796
38. Lowe LH, Bailey Z (2011) State-of-the-art cranial sonography: Part 2, pitfalls and variants. AJR Am J Roentgenol 196:1034–1039
39. Correa FF, Lara C, Bellver J et al (2006) Potential pitfalls in fetal neurosonography. Prenat Diagn 26:52–56
40. Enríquez G, Correa F, Lucaya J et al (2003) Potential pitfalls in cranial sonography. Pediatr Radiol 33:110–117
41. Tomà P, Granata C (2015) Brain sonography. In: Rossi A (ed) Pediatric neuroradiology. Springer, Berlin, pp 1–53
42. Tu S, Doherty D, Schilmoeller KJ, Schilmoeller GL (2009) Agenesis of the corpus callosum: a literature review. Int Rev Res Ment Retard 38:171–193
43. Schell-Apacik CC, Wagner K, Bihler M et al (2008) Agenesis and dysgenesis of the corpus callosum: clinical, genetic and neuroimaging findings in a series of 41 patients. Am J Med Genet A 146A: 2501–2511
44. Kazi AI, Iqbal Y, Kazi SE (2015) Antenatal diagnosis of corpus callosal agenesis. J Fetal Med 2:87–90
45. Innocenti GM, Caminiti R, Hof PR (2010) Fiber composition in the planum temporale sector of the corpus callosum in chimpanzee and human. Brain Struct Funct 215:123–128
46. Hines M, Chiu L, McAdams LA et al (1992) Cognition and the corpus callosum: verbal fluency, visuospatial ability, and language lateralization related to midsagittal surface areas of callosal subregions. Behav Neurosci 106:3–14
47. Liu F, Cao S, Liu J et al (2013) Ultrasound measurement of the corpus callosum and neural development of premature infants. Neural Regen Res 8:2432–2440
48. Youssef A, Ghi T, Pilu G (2013) How to image the fetal corpus callosum. Ultrasound Obstet Gynecol 42:718–720
49. Rajmohan V, Mohandas E (2007) The limbic system. Indian J Psychiatry 49:132–139
50. Swenson RS, Gulledge AT (2017) The cerebral cortex. In: Conn PM (ed) Conn's translational neuroscience. Elsevier, Philadelphia, pp 263–288
51. Johns P (2014) Functional neuroanatomy. In: Clinical neuroscience. Churchill Livingstone, London, pp 27–47
52. Chu RM, Black KL (2012) Current surgical management of high-grade gliomas. In: Quiñones-Hinojosa A (ed) Schmidek and sweet operative neurosurgical techniques, 6th edn. Elsevier Saunders, Philadelphia, pp 105–110
53. Japee S, Holiday K, Satyshur MD et al (2015) A role of right middle frontal gyrus in reorienting of attention: a case study. Front Syst Neurosci 9:23
54. Petrides M, Pandya DN (2012) The frontal cortex. In: Jürgen KM, Paxinos G (eds) The human nervous system, 3rd edn. Elsevier, Philadelphia, pp 988–1011
55. Tyler LK, Marslen-Wilson WD, Randall B et al (2011) Left inferior frontal cortex and syntax: function, structure and behaviour in patients with left hemisphere damage. Brain 134:415–431
56. Pooh RK, Machida M, Nakamura T et al (2019) Increased Sylvian fissure angle as early sonographic sign of malformation of cortical development. Ultrasound Obstet Gynecol 54:199–206
57. Abdel Razek AAK, Kandell AY, Elsorogy LG et al (2009) Disorders of cortical formation: MR imaging features. AJNR Am J Neuroradiol 30:4–11
58. Kiernan JA (2012) Anatomy of the temporal lobe. Epilepsy Res Treat 2012:176157
59. ten Donkelaar HJ, Tzourio-Mazoyer N, Mai JK (2018) Toward a common terminology for the gyri and sulci of the human cerebral cortex. Front Neuroanat 12:93
60. Rolston JD, Englot DJ, Benet A et al (2015) Frontal operculum gliomas: language outcome following resection. J Neurosurg 122: 725–734
61. Stephani C, Fernandez-Baca Vaca G, Maciunas R et al (2011) Functional neuroanatomy of the insular lobe. Brain Struct Funct 216:137–149
62. Uddin LQ, Nomi JS, Hébert-Seropian B et al (2017) Structure and function of the human insula. J Clin Neurophysiol 34:300–306
63. Onitsuka T, Shenton ME, Salisbury DF et al (2004) Middle and inferior temporal gyrus gray matter volume abnormalities in chronic schizophrenia: an MRI study. Am J Psychiatry 161:1603–1611
64. Weiner KS, Zilles K (2016) The anatomical and functional specialization of the fusiform gyrus. Neuropsychologia 83:48–62
65. Aminoff EM, Kveraga K, Bar M (2013) The role of the parahippocampal cortex in cognition. Trends Cogn Sci 17:379–390
66. Carrasco R, Pascual JM, Navas M et al (2009) Kernohan-Woltman notch phenomenon caused by an acute subdural hematoma. J Clin Neurosci 16:1628–1631
67. Rhoton AL Jr (2002) The cerebrum. Neurosurgery 51:S1–S51
68. Tanriover N, Rhoton AL Jr, Kawashima M et al (2004) Microsurgical anatomy of the insula and the Sylvian fissure. J Neurosurg 100:891–922
69. Buneo CA, Andersen RA (2006) The posterior parietal cortex: sensorimotor interface for the planning and online control of visually guided movements. Neuropsychologia 44:2594–2606
70. Grill-Spector K, Kourtzi Z, Kanwisher N (2001) The lateral occipital complex and its role in object recognition. Vis Res 41:1409–1422
71. Nagy K, Greenlee MW, Kovács G (2012) The lateral occipital cortex in the face perception network: an effective connectivity study. Front Psychol 3:141